

hep-ph/9806340  
PSU/TH/200

## Tests of Factorization in Diffractive Charm Production and Double Pomeron Exchange

Lyndon Alvero, John C. Collins and J. J. Whitmore

*Physics Department, Pennsylvania State University  
104 Davey Lab., University Park, PA 16802-6300, U.S.A.*  
(10 June 1998)

### Abstract

We present predictions for the diffractive production of heavy quarks in deep-inelastic scattering and hadron-hadron collisions and for double diffractive dijet production in hadron-hadron collisions. With the assumption of hard scattering factorization, the predictions are made using diffractive parton densities that we have previously fitted to HERA data. Comparisons of our predictions with preliminary data from HERA and the Tevatron indicate that factorization is obeyed in diffractive DIS but fails in hadron-induced processes.

13.60.Hb 13.60.-r 13.85.Qk 13.87.-a

## I. INTRODUCTION

In a previous paper [1], we obtained diffractive parton densities by fitting diffractive deep inelastic scattering (DIS) and photoproduction data from HERA, and then we used these to predict diffractive production of  $W$ 's and dijets at the Tevatron. The underlying principle behind these calculations was the notion of hard scattering factorization, a property which we aimed to test.

A factorization theorem has been proven [2] for diffractive DIS and direct photoproduction processes. The proof establishes the universality of diffractive parton densities for the class of processes to which the theorem applies. This means that one may extract the parton densities from a subset of data, and then, using these same densities, reliably predict other diffractive DIS and direct photoproduction distributions. The results of our work in [1] are consistent with this theorem.

In contrast, no factorization theorem has been established for diffractive hadron-hadron processes, and in fact, there have been several arguments put forward in favor of nonfactorization [3,4] in this case. Again, our results in [1] were consistent with this, when we compared our predictions for hadron-hadron processes to data.

In this paper, we seek to further extend our tests of factorization. Using the same diffractive parton densities that we extracted in [1], we present calculations of cross sections for one process where factorization is predicted to be valid—diffractive heavy quark production from DIS—and for two processes where factorization is predicted to fail—diffractive heavy quark production in  $p\bar{p}$  interactions, and diffractive dijet production via double Pomeron exchange. We will compare our predictions with preliminary data from HERA [5,6] and the Tevatron [7,8].

Apart from the general desire to test hard-scattering factorization, a particular motivation for studying diffractive DIS charm production is that we expect charm production to be a substantial fraction of the diffractive DIS cross section. (Recall that in inclusive DIS, the charm structure function  $F_2^{c\bar{c}}$  is  $\sim 25\%$  of the inclusive  $F_2$ .) Moreover, since open charm production is dominated by the photon-gluon fusion process, it also provides a good test of the normalization of the diffractive gluon density. A particular result of our work in [1] was that the diffractive gluon density is much larger than the diffractive quark density. This was most strongly driven by the photoproduction data. The hadron-induced processes that we study in this paper are also highly sensitive to the diffractive gluon density.

The paper is organized as follows. In section II, we discuss the diffractive parton densities and cross section formulae that we will use in the calculations. Our numerical results are then presented and discussed in relation to preliminary data in section III. We then summarize our findings and give our conclusions in section IV.

## II. CROSS SECTIONS

Since our goal is to test hard scattering factorization, we will use, in our calculations of the diffractive cross sections, the parton densities which we previously obtained [1] from fits to diffractive DIS and photoproduction data from ZEUS and H1. Similar fits were also obtained independently in [9,10], using only data from ZEUS. Note that there have also been previous fits to diffractive DIS data alone [11].

In [1], where we assumed that the diffractive parton densities can be adequately represented as a Pomeron flux factor times parton densities in the Pomeron, the fits are labeled A, B, C, D and SG. In fits A, B, C and D, the parton densities in the Pomeron all have the form,

$$\begin{aligned}\beta f_{q/\mathbb{P}}(\beta, Q_0) &= a_q [\beta(1 - \beta) + \tilde{a}_q (1 - \beta)^2], \\ \beta f_{g/\mathbb{P}}(\beta, Q_0) &= a_g \beta(1 - \beta),\end{aligned}\quad (1)$$

at an initial scale  $Q_0 = 2$  GeV, but with different constraints on the parameters. For example, in parameterizations A and C we required that there be no gluons in the initial parton densities, i.e.,  $a_g = 0$ . The super-high-glue fit, SG, has the same form of quark density as in Eq. (1) but with a gluon density that is peaked near  $\beta = 1$  and is given by

$$\beta f_{g/\mathbb{P}}(\beta, Q_0) = a_g \beta^8 (1 - \beta)^{0.3}. \quad (2)$$

The appropriate Pomeron flux factor to use with the above parton densities is one due to Donnachie and Landshoff [12]:

$$f_{\mathbb{P}/p}^{\text{DL}}(x_{\mathbb{P}}) = \int_{-1}^0 dt \frac{9\beta_0^2}{4\pi^2} \left[ \frac{4m_p^2 - 2.8t}{4m_p^2 - t} \left( \frac{1}{1 - t/0.7} \right)^2 \right]^2 x_{\mathbb{P}}^{1-2\alpha(t)}, \quad (3)$$

where  $m_p$  is the proton mass,  $\beta_0 \simeq 1.8$  GeV $^{-1}$  is the Pomeron-quark coupling and  $\alpha(t) = \alpha_{\mathbb{P}} + 0.25t$  is the Pomeron trajectory.

The explicit parameters for our fits are presented in Table I. Note that fits A and C have low gluon content (i.e., gluons are only produced via evolution) while fits B, D and SG contain large amounts of initial gluons. In [1], we found that only the high-glue fits are able to fit the photoproduction data while the low-glue fits badly underestimate the same data. All five parameterizations are in reasonable agreement with the DIS data, at least as regards normalization.

Our motivation for working with fits that do not in fact fit all the data is that the gluon distributions that are needed to provide good fits to photoproduction data are an order of magnitude above the quark distributions. This is quite unlike the usual inclusive parton densities in the proton. Thus, a comparison of results obtained with the low-glue and high-glue fits should dramatically distinguish those processes that are particularly sensitive to the diffractive gluon density from those that are merely sensitive to the gluon densities in their finer details.

### A. Heavy quarks in DIS

We compute the total cross section for diffractive production of heavy quarks in DIS with the usual formula

$$\sigma = \sum_a \int dx_a dx_{\mathbb{P}} f_{a/\mathbb{P}}(x_a, \mu) f_{\mathbb{P}/p}(x_{\mathbb{P}}) \hat{\sigma}_{a\gamma^*}, \quad (4)$$

where  $x_a$  and  $x_{\mathbb{P}}$  are momentum fractions of parton  $a$  and the Pomeron, respectively,  $f_{a/\mathbb{P}}(x_a, \mu)$  is the distribution function at scale  $\mu$  of parton  $a$  in the Pomeron,  $f_{\mathbb{P}/p}(x_{\mathbb{P}})$

Fit	$a_q$	$a_g$	$\tilde{a}_q$
A	$0.240 \pm 0.006$	0	0
B	$0.239 \pm 0.006$	$4.5 \pm 0.5$	0
C	$0.249 \pm 0.011$	0	$-0.031 \pm 0.029$
D	$0.292 \pm 0.013$	$9.7 \pm 1.7$	$-0.159 \pm 0.029$
SG	$0.225 \pm 0.008$	$7.4 \pm 2.2$	0

TABLE I. Fit parameters and associated errors for the diffractive parton densities with  $\alpha_{\mathbb{P}} = 1.14$  as presented in [1].

is the Pomeron flux factor and  $\hat{\sigma}_{a\gamma^*}$  is the coefficient function for parton-virtual photon ( $\gamma^*$ ) scattering. The next-to-leading order form of this function may be found in [13]. The sum in Eq. (4) runs over all active parton flavors.

The calculation that we have used is based on HVQDISv1.1 by B. W. Harris and J. Smith [14] which computes inclusive (i.e., without the diffractive requirement), fully differential heavy quark distributions in DIS both to leading (LO) and next-to-leading order (NLO). A Peterson fragmentation routine is built-in and can be applied to the final state heavy quark four-vectors to simulate hadronization effects. We modified this calculation to compute diffractive cross sections using the diffractive parton densities obtained in [1].

## B. Heavy quarks in hadron collisions

The cross sections for heavy quark pair ( $Q\bar{Q}$ ) production in  $p\bar{p}$  collisions for the case when the  $\bar{p}$  diffracts are calculated using

$$\sigma_{Q\bar{Q}} = \sum_{a,b} \int dx_a dx_b dx_{\mathbb{P}} f_{\mathbb{P}/\bar{p}}(x_{\mathbb{P}}) f_{b/\mathbb{P}}(x_b, \mu) f_{a/p}(x_a, \mu) \hat{\sigma}_{ab \rightarrow Q\bar{Q}}(x_a x_b s, m_Q^2, \mu^2), \quad (5)$$

where  $f_{a/p}(x_a, \mu)$  is the proton parton distribution function,  $s$  is the center of mass energy squared,  $m_Q$  is the heavy quark mass and  $\hat{\sigma}_{ab \rightarrow Q\bar{Q}}$  is the partonic hard scattering function for heavy quark pair production. The analytic expressions for this function up to NLO are given in [15].

It is useful to present the above cross section as a fraction of the inclusive cross section. Thus, we will also compute the diffractive rate  $R = \sigma_{Q\bar{Q}} / \sigma_{Q\bar{Q}}^{\text{incl}}$ , where

$$\sigma_{Q\bar{Q}}^{\text{incl}} = \sum_{a,b} \int dx_a dx_b f_{a/p}(x_a, \mu) f_{b/\bar{p}}(x_b, \mu) \hat{\sigma}_{ab \rightarrow Q\bar{Q}}(x_a x_b s, m_Q^2, \mu^2). \quad (6)$$

### C. Dijets via double Pomeron exchange

For the production of dijets via double Pomeron exchange in  $p\bar{p}$  collisions, we compute the cross section by using

$$\sigma^{\text{DPE}} = \sum_{a,b} \int dx_a dx_b dx_{\mathbb{P}/p} dx_{\mathbb{P}/\bar{p}} f_{\mathbb{P}/p}(x_{\mathbb{P}/p}) f_{a/\mathbb{P}}(x_a, \mu) f_{\mathbb{P}/\bar{p}}(x_{\mathbb{P}/\bar{p}}) f_{b/\mathbb{P}}(x_b, \mu) \hat{\sigma}_{ab}, \quad (7)$$

where  $\hat{\sigma}_{ab}$  is the partonic  $2 \rightarrow 2$  scattering function. The LO expressions for  $\hat{\sigma}_{ab}$  may be found in [16].

We will also compute the ratio of the above double diffractive cross section to that for single diffraction ( $\sigma^{\text{SD}}$ ). The latter, assuming the  $\bar{p}$  diffracts, is calculated with the formula

$$\sigma^{\text{SD}} = \sum_{a,b} \int dx_a dx_b dx_{\mathbb{P}} f_{a/p}(x_a, \mu) f_{\mathbb{P}/\bar{p}}(x_{\mathbb{P}}) f_{b/\mathbb{P}}(x_b, \mu) \hat{\sigma}_{ab}. \quad (8)$$

## III. RESULTS AND COMPARISONS WITH DATA

In computing the diffractive cross sections, we used the diffractive parton densities discussed in section II. These are evolved using full NLO QCD, via the CTEQ package [17], from the initial scale  $Q_0$  to the appropriate scale in the particular calculation.

For the calculations involving heavy quarks, NLO hard scattering matrix elements [15] were used together with a two-loop running coupling  $\alpha_s$ . To be consistent with the renormalization scheme used in [15], one needs to use the coupling  $\alpha_s$  which is valid for three and four flavors for charm ( $c$ ) and bottom ( $b$ ) production, respectively. At NLO, the matching condition between the 3- and 4-flavor couplings at  $\mu = m_c$  is that the coupling is continuous, and similarly for the transition from 4 to 5 active flavors — see [18]. For consistency in the calculations of  $\sigma_{Q\bar{Q}}^{\text{inel}}$ , we also used proton parton densities with the appropriate number of flavors [19] in the fixed flavor scheme [20]: CTEQ4F3 (CTEQ4F4) for charm (bottom) production.

### A. Diffractive charm production at HERA

Both the H1 [5] and ZEUS [6] collaborations have reported preliminary data on diffractive charm production in deep inelastic scattering of 27.5 GeV positrons and 820 GeV protons. They studied charm quark production, by tagging  $D^*$  mesons through their decay, via the process

$$e^+ + p \rightarrow e^+ + p + (D^{*\pm} \rightarrow (D^0 \rightarrow K^-\pi^+) \pi^\pm) + X. \quad (9)$$

#### 1. H1 data

H1 has measured a preliminary cross section for diffractive  $D^*$  production shown in the last column of Table II. This is subject to the following cuts:  $10 \text{ GeV}^2 < Q^2 < 100 \text{ GeV}^2$ ,

	A	B	C	D	SG	H1 data
$\sigma$	4.22	196	4.15	419	70.3	$380^{+150}_{-120}$ (stat.) $^{+140}_{-110}$ (syst.)

TABLE II. Diffractive  $D^*$  cross sections (pb) in DIS using H1 cuts. The last column shows the preliminary measurement by H1 [5].

	$x_{\mathbb{P}}^{\max} = 0.01$	$x_{\mathbb{P}}^{\max} = 0.05$	$x_{\mathbb{P}}^{\max} = 0.1$
A	0.74	5.15	8.67
B	76.7	242	315
C	0.75	5.09	8.46
D	165	518	670
SG	43.2	87.4	105
ZEUS data	$604 \pm 171$ (stat.) $^{+295}_{-178}$ (syst.)		

TABLE III. Diffractive  $D^*$  cross sections (pb) in DIS using ZEUS cuts and for several different limits on  $x_{\mathbb{P}}$ . The bottom row shows the preliminary measurement by ZEUS [6].

$p_T(D^{*\pm}) > 1$  GeV,  $0.06 < y < 0.6$ ,  $x_{\mathbb{P}} < 0.05$  and  $|\eta(D^{*\pm})| < 1.25$ , where  $Q^2$  is the photon virtuality,  $y$  is the fractional energy loss of the incident  $e^+$  in the proton rest frame while  $p_T$  and  $\eta$  are the transverse momentum and pseudorapidity, respectively, of the  $D^*$  meson. These data include proton dissociation with masses up to 1.6 GeV.

The NLO cross sections that we calculated with the same cuts are also given in Table II. These values were obtained with Peterson fragmentation switched on in the code with  $\epsilon_c = 0.035$  and the probability for the charm to fragment into a  $D^*$  meson,  $P(c \rightarrow D^*)$ , set equal to 0.26. The renormalization and factorization scales in Eq. (4) were both set to  $\mu = \sqrt{Q^2 + 4m_c^2}$ , where the mass of the charm quark,  $m_c$ , is set equal to 1.5 GeV.

We see that with the low-glue fits A and C, our predicted cross sections are two orders of magnitude smaller than the data. With fits B and SG, our cross sections are about two and five times smaller than the central data value but within the errors. Fit D, which provided our best fit to the DIS and photoproduction cross sections, yields a diffractive charm cross section which is in best agreement with the data, being within 10% of the central value.

## 2. ZEUS data

For the same process, the cross section obtained by ZEUS, corrected for a  $(31 \pm 13)\%$  double dissociation contribution, is given in the bottom row of Table III. The following experimental cuts apply for this measurement:  $10 \text{ GeV}^2 < Q^2 < 80 \text{ GeV}^2$ ,  $p_T(D^{*\pm}) > 1 \text{ GeV}$ ,  $0.04 < y < 0.7$ ,  $|\eta(D^{*\pm})| < 1.5$ , and  $\eta_{\max} < 2$ .

Using the same cuts, we derive the cross sections shown in Table III. We used the same fragmentation parameters and choice of scale as in the calculations for comparison with the H1 data. Since the ZEUS data have an  $\eta_{\max}$  cut, it is not clear what limit to impose on  $x_{\mathbb{P}}$ . Hence, we have chosen several different values, as shown.

We find that if we use the cut  $x_{\mathbb{P}} < 0.01$ , the predictions badly underestimate the data. Using cuts of 0.05 and 0.1, the predictions obtained with the low-glue fits A and C are still one to two orders of magnitude smaller than the data. The predictions using the high-glue fits B, D and SG have better agreement, with those obtained from D being closest to the data.

### 3. Sizes of predictions

We make several remarks on the relative sizes of our predictions for this process. The cross sections derived with the low-glue fits (A and C) are from 16 to about 100 times smaller than those obtained from the high-glue fits B, D and SG. This large discrepancy is due to the fact that the production of heavy quarks in DIS is dominated by the  $\gamma^* - g$  channel, with quark contributions entering only at next-to-leading order. With fits A and C, gluons are generated only via evolution of the parton densities. Therefore, the predictions using fits A or C are suppressed by at least a factor of  $\alpha_s$  relative to those with the high-glue fits. Furthermore, another factor of 10 suppression results from the quark coefficients in Table I being an order of magnitude smaller than the gluon coefficients.

Among the high-glue fits, the cross section using SG is smallest. This indicates that, for this process, the bulk of the contribution comes from partons with momentum fractions ( $x$ ) that are moderately far from unity; the gluon density of SG dominates that of B or D only in the region  $x \sim 1$ . The cross sections using fits B and D have about a factor of two difference. This is due to the gluon coefficient  $a_g$  for D being about twice that for B and the dominance of gluon-induced scattering in this process.

### 4. Differential cross sections

Figure 1 shows our predicted differential cross sections using H1 cuts plotted as functions of  $W$  (the center-of-mass energy of the virtual photon-proton system),  $Q^2$ ,  $p_T(D^*)$ ,  $\eta(D^*)$  and  $x_{\mathbb{P}}$ . The same comments apply regarding the relative sizes of the predictions for each distribution as those made above. The plots strongly illustrate how well diffractive charm production in DIS can determine the gluon density as evidenced by the large difference between the predictions using the realistic high-glue fits (D, B and SG) and the low-glue ones (A and C).

## B. Heavy quark production from hadrons

At this time, there are no data available for comparison with our predictions although there is a preliminary report from CDF [21] which quotes that “ $(0.18 \pm 0.03)\%$  of central high- $p_T b/c$  are diffractively produced” in  $p\bar{p}$  interactions at  $\sqrt{s} = 1800$  GeV. One may thus expect that data on diffractive heavy quark production will soon become available. It is useful, therefore, to make some predictions to study the differences between the diffractive parton densities.

For open heavy flavor ( $Q\bar{Q}$ ) production from  $p\bar{p}$  interactions at  $\sqrt{s} = 1.8$  TeV, we obtained the NLO diffractive cross sections (assuming that only the  $\bar{p}$  diffracts) shown in

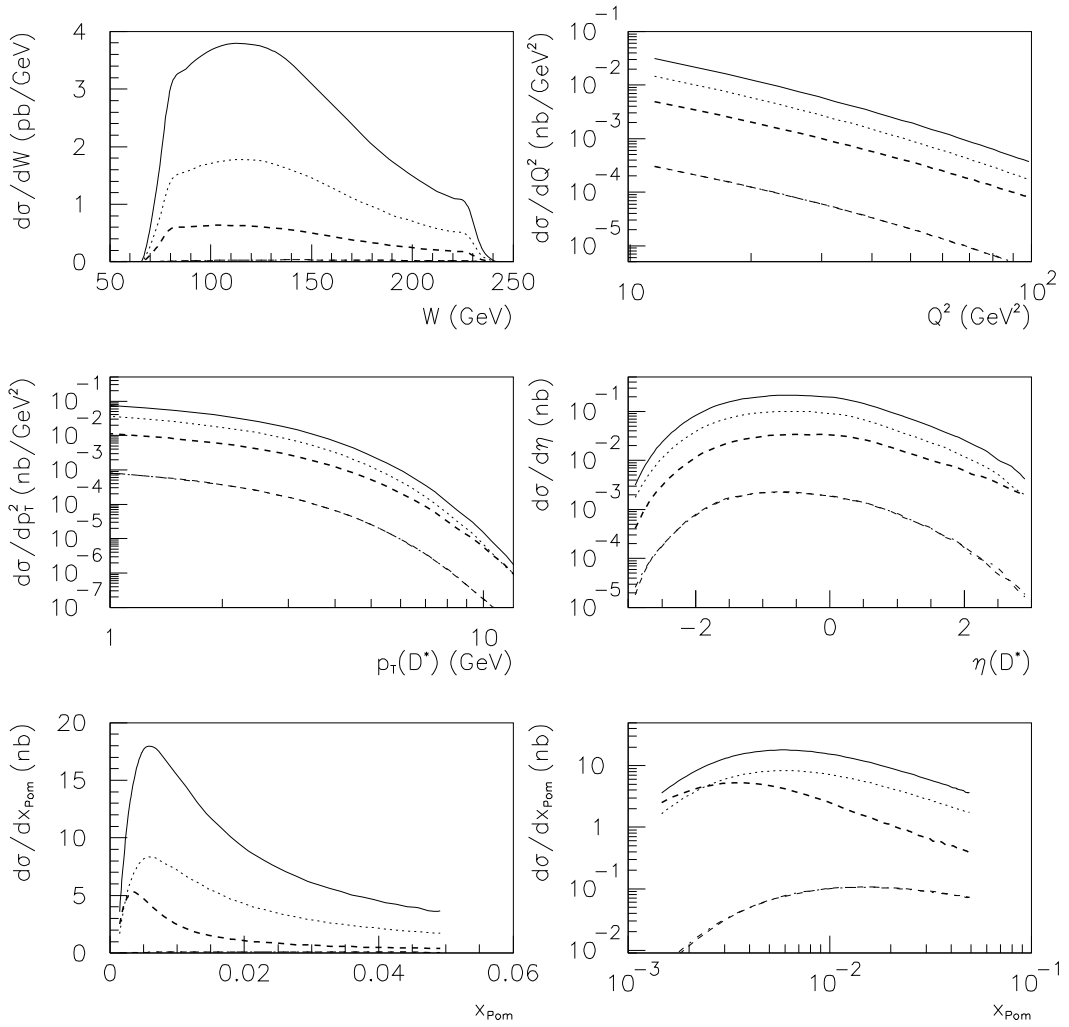


FIG. 1. Various distributions for diffractive  $D^*$  production in DIS using H1 cuts. Solid curves are for predictions obtained with fit D, dotted for those with fit B, heavy dashed for fit SG, dot-dashed for fit C and dashed for fit A. (The last two lie almost on top of each other.) Only fits B,D and SG are to be regarded as realistic predictions. The two plots at the bottom are identical except for the choice of scale for the axes.

		$x_{\mathbb{P}}^{\max} = 0.01$		$x_{\mathbb{P}}^{\max} = 0.05$		$x_{\mathbb{P}}^{\max} = 0.1$	
		$\sigma_{Q\bar{Q}}$	$R$	$\sigma_{Q\bar{Q}}$	$R$	$\sigma_{Q\bar{Q}}$	$R$
$Q = \text{ charm}$	A	5.2	0.2%	8.6	0.4%	10.5	0.5%
	B	194	8.8%	323	14.6%	390	17.7%
	C	5.0	0.2%	8.1	0.4%	9.9	0.5%
	D	414	18.7%	689	31.2%	831	37.6%
	SG	69.1	3.1%	108	4.9%	128	5.8%
$Q = \text{ bottom}$	A	0.1	0.1%	0.2	0.3%	0.3	0.5%
	B	1.7	2.6%	4.5	6.9%	6.4	9.9%
	C	0.1	0.1%	0.2	0.3%	0.3	0.5%
	D	3.5	5.4%	9.5	14.6%	13.5	20.8%
	SG	0.8	1.2%	1.9	2.9%	2.6	3.9%

TABLE IV. Diffractive cross sections  $\sigma_{Q\bar{Q}}$  ( $\mu\text{b}$ ) and rates  $R = \sigma_{Q\bar{Q}}/\sigma_{Q\bar{Q}}^{\text{incl}}$  for open charm and bottom production at the Tevatron using several different cuts on  $x_{\mathbb{P}}$ . These values are valid for the case when only the  $\bar{p}$  diffracts.

Table IV. The corresponding rates,  $R = \sigma_{Q\bar{Q}}/\sigma_{Q\bar{Q}}^{\text{incl}}$ , are also shown in the same table. We used  $m_c = 1.5$  GeV and  $m_b = 4.5$  GeV for the charm and bottom quark masses, respectively, and set the scale  $\mu$  in Eqs. (5,6) to the heavy quark mass.

As in the case of heavy quark production in DIS, the predicted cross sections using the (unrealistic) low-glue fits A and C are one to two orders of magnitude smaller, depending on the cut on  $x_{\mathbb{P}}$  used, than those obtained with fits B, D and SG. Again, this is because most of the cross section for this process results from gluon-induced ( $g - g$  and  $g - q$ ) scattering.

From Table IV, we see that for charm (bottom) production, the predicted diffractive cross sections using the high-glue fits are about 3% to 40% (1% to 20%) of the inclusive cross section. The low-glue fits result in much smaller rates: 0.2% to 0.5% and 0.1% to 0.5% for charm and bottom production, respectively.

### C. Dijets via double Pomeron exchange at the Tevatron

CDF has preliminary data [7,8] on double diffractive dijet production from  $p\bar{p}$  interactions at  $\sqrt{s} = 1.8$  TeV which are characterized by central dijets bounded by rapidity gaps near the direction of each incoming hadron. They used a Roman pot to trigger on the diffracting antiproton and tagged on rapidity gaps along the direction of the diffracting proton. The measured cross section [7] for dijets with transverse energy  $E_T > 7$  GeV and cuts of  $0.05 < x_{\mathbb{P}/\bar{p}} < 0.1$  and  $0.015 < x_{\mathbb{P}/p} < 0.035$ , where  $x_{\mathbb{P}/h}$  is the fractional momentum lost by the diffracting hadron  $h$ , is shown in the last column of Table V.

There also exist data on the double diffractive cross section  $\sigma^{\text{DPE}}$  expressed as a fraction of the single diffractive cross section  $\sigma^{\text{SD}}$ . The fraction  $\sigma^{\text{DPE}}/\sigma^{\text{SD}}$  measured by CDF [8] is shown in Table V. In this case, the denominator  $\sigma^{\text{SD}}$  is the cross section for production of dijets with  $E_T > 7$  GeV and a cut  $0.05 < x_{\mathbb{P}/\bar{p}} < 0.1$  (obtained with a Roman pot trigger on the diffracting antiproton).

	A	B	C	D	SG	Preliminary CDF data
$\sigma^{\text{DPE}}$	10.1	898	9.82	3713	206	$13.6 \pm 2.8 \text{ (stat.)} \pm 2.0 \text{ (syst.)}$
$\sigma^{\text{DPE}}/\sigma^{\text{SD}}$	0.18%	1.66%	0.19%	3.42%	0.89%	$[0.17 \pm 0.036 \text{ (stat.)} \pm 0.024 \text{ (syst.)}] \%$

TABLE V. Dijet cross sections in  $p\bar{p}$  interactions via double Pomeron exchange using CDF cuts. The first row shows the cross section (nb) while the second row presents the rates expressed as a fraction of the single diffractive cross section ( $\sigma^{\text{SD}}$ ). The last column shows the CDF preliminary measurements.

The cross sections  $\sigma^{\text{DPE}}$  and ratios  $\sigma^{\text{DPE}}/\sigma^{\text{SD}}$  that we obtain using the same cuts and the diffractive parton densities shown in section II are also presented in Table V. In our calculations, we set the scale  $\mu$  in Eqs. (7,8) equal to  $E_T$ .

Compared to the data, we find that the predicted cross section  $\sigma^{\text{DPE}}$  and ratio  $\sigma^{\text{DPE}}/\sigma^{\text{SD}}$  obtained with the low-glue fits, A and C, agree well with the data. However, as we have seen, these fits substantially underestimate diffractive photoproduction and diffractive charm production. With the realistic high-glue fits B, D and SG, the predictions badly overestimate the data, being one to two orders of magnitude larger.

The relative sizes of the predicted cross sections in Table V can be explained in the following way. As in the case of heavy quark production, dijet production is dominated by gluon-induced scattering at the parton level. However, in this case, quarks do contribute at the leading order. Even then, the cross sections using fits A and C are much smaller relative to those obtained with the fits B, D and SG than in the heavy quark case (see Tables II, III and IV). The reason is that in the double Pomeron exchange cross section, there is an extra factor of the gluon density for the second Pomeron. Fits A and C are then expected to produce smaller cross sections because they can only supply gluons for the hard scattering via evolution. Similarly, the factor of four difference between the results for fits B and D is a consequence of fit D having about twice as much initial gluon as B.

#### IV. CONCLUSIONS

We have presented diffractive heavy quark and dijet cross sections calculated with the assumption of hard scattering factorization. Diffractive parton densities that were fitted [1] to DIS and photoproduction data from HERA were used in these calculations. In [1], our best fit to the data resulted in fit D.

We find that in the case of diffractive  $D^*$  production, the predicted cross sections using the best-fit parton densities, fit D, also have the best agreement with the data. This strongly supports the notion of hard scattering factorization for diffractive lepton-hadron processes.

For heavy quark production from  $p\bar{p}$  collisions and assuming only the  $\bar{p}$  diffracts, we obtained rates  $R = \sigma_{Q\bar{Q}}/\sigma_{Q\bar{Q}}^{\text{inel}}$ , using the high-glue fits, from 3% to 40% and 1% to 20% for open charm and bottom production, respectively. The rates obtained with the low-glue fits are less than 1% for either charm or bottom production. It will be interesting to see how well these figures compare when data from the Tevatron become available.

Our results for diffractive dijet production at the Tevatron indicate a breakdown of factorization for diffractive hadron-hadron processes. The predicted double Pomeron exchange

cross sections  $\sigma^{\text{DPE}}$  with the high-glue fits are factors of 10-100 times larger than data. Similar results are obtained when comparing the ratio  $\sigma^{\text{DPE}}/\sigma^{\text{SD}}$  with data. Only the low-glue fits, which do not fit diffractive photoproduction data at all, yield numbers that agree well with the data.

#### ACKNOWLEDGMENTS

This work was supported in part by the U.S. Department of Energy under grant number DE-FG02-90ER-40577, and by the U.S. National Science Foundation. We thank B. Harris and J. Smith for providing us with the codes for HVQDISv1.1 and for helpful discussions. L. Alvero would also like to thank A. Berera for discussions.

## REFERENCES

- [1] L. Alvero, J.C. Collins, J. Terron and J.J. Whitmore, “Diffractive Hadronic Production of Jets and Weak Bosons”, hep-ph 9805268.
- [2] J.C. Collins, Phys. Rev. **D57**, 3051 (1998), hep-ph/9709499.
- [3] J.C. Collins, L. Frankfurt and M. Strikman, Phys. Lett. **B307**, 161 (1993), hep-ph/9212212; A. Berera and J.C. Collins, Nucl. Phys. **B474**, 183 (1996), hep-ph/9509258.
- [4] P.V. Landshoff and J.C. Polkinghorne, Nucl. Phys. **B33**, 221 (1971) and **B36**, 642 (1972); F. Henyey and R. Savit, Phys. Lett. **52B**, 71 (1974); J.L. Cardy and G.A. Winbow, Phys. Lett. **52B**, 95 (1974); C. DeTar, S.D. Ellis and P.V. Landshoff, Nucl. Phys. **B87**, 176 (1975).
- [5] H1 Collaboration, “A Measurement of the Production of  $D^{*\pm}$  Mesons in Deep-Inelastic Diffractive Interactions at HERA”, contribution pa02-060 to ICHEP96, Warsaw, July 1996.
- [6] ZEUS Collaboration, “ $D^{*\pm}$  Meson Production in Deep Inelastic Scattering at HERA with the ZEUS Detector”, contribution N-643 to EPS97, Jerusalem, August 1997.
- [7] M.G. Albrow, CDF Collaboration, Fermilab-Conf-98/138-E, “Di-jet Production by Double Pomeron Exchange in CDF”, contribution to LISHEP 98, Rio de Janeiro, February 1998.
- [8] K. Goulianos, CDF Collaboration, Proceedings of the XXXIIInd Rencontre de Moriond, “QCD '97 and High Energy Hadronic Interactions”, ed. J. Tran Thanh Van (Editions Frontières), p. 447.
- [9] ZEUS Collaboration, “Diffractive Dijet Cross Sections and Rapidity Gap Between Jets in Hard Photoproduction at HERA”, preprint N-648/N-655, contribution to EPS97, Jerusalem, Aug. 1997, [http://www-zeus.desy.de/plots97/eps97/et\\_difdijF.ps](http://www-zeus.desy.de/plots97/eps97/et_difdijF.ps).
- [10] ZEUS Collaboration, “Diffractive Dijet Cross Sections in Photoproduction at HERA”, hep-ex/9804013.
- [11] C. Adloff *et al.*, H1 Collaboration, Z. Phys. **C76**, 613 (1997); T. Gehrman and W.J. Stirling, Z. Phys. **C70**, 89 (1996); Z. Kunszt and W.J. Stirling, “Hard diffractive scattering: partons and QCD”, in Deep Inelastic Scattering and Related Phenomena (DIS-96): Eds. G. D'Agostini and A. Nigro (World Scientific, 1997).
- [12] A. Donnachie and P.V. Landshoff, Phys. Lett. **B191**, 309 (1987); Nucl. Phys. **B303**, 634 (1988).
- [13] B.W. Harris and J. Smith, Nucl. Phys. **B452**, 109 (1995).
- [14] B.W. Harris and J. Smith, Phys. Rev. **D57**, 2806 (1998).
- [15] P. Nason, S. Dawson and R.K. Ellis, Nucl. Phys. **B327**, 49 (1989).
- [16] E. Eichten, I. Hinchliffe, K. Lane and C. Quigg, Rev. Mod. Phys. **56**, 579 (1984); **58**, 1065 (1986).
- [17] The CTEQ evolution package can be obtained from  
<http://www.phys.psu.edu/~cteq/>.
- [18] J. Collins, F. Wilczek, and A. Zee, Phys. Rev. **D18**, 242 (1978);  
 Particle Data Group, R.M. Barnett et al., *Review of Particle Physics*, Phys. Rev. **D54**, 1 (1996).  
 K.G. Chetyrkin, B.A. Kniehl, and M. Steinhauser, Phys. Rev. Lett. **79**, 2184 (1997), hep-ph/9706430; K.G. Chetyrkin, B.A. Kniehl, and M. Steinhauser, Nucl. Phys. **B510**, 61 (1998), hep-ph/9708255, and references therein.

- [19] M.A.G. Aivazis, J.C. Collins, F.I. Olness, and W.-K. Tung, Phys. Rev. **D50**, 3102 (1994), hep-ph/9312319; J.C. Collins and W.-K. Tung, Nucl. Phys. **B278**, 934 (1986).
- [20] H.L. Lai and W.K. Tung, Z. Phys. **C74**, 463 (1997).
- [21] M.G. Albrow, CDF Collaboration, Fermilab-Conf-97/361-E, “Hard Diffraction in CDF”, Proceedings of 7th Blois Workshop on Elastic and Diffractive Scattering, Seoul, June 1997.